



Cite this: *RSC Adv.*, 2018, 8, 30994

Coordination properties of *N,N'*-bis(5-methylsalicylidene)-2-hydroxy-1,3-propanediamine with d- and f-electron ions: crystal structure, stability in solution, spectroscopic and spectroelectrochemical studies†

Malgorzata T. Kaczmarek,[✉] Monika Skrobanska, Michal Zabiszak, Monika Wałęsa-Chorab,[✉] Maciej Kubicki[✉] and Renata Jastrzab[✉]

Template reaction between 5-methylsalicylaldehyde and 2-hydroxy-1,3-propanediamine in the presence of copper ion led to dinuclear and mononuclear copper(II) complexes [Cu₂L(CH₃COO)(CH₃OH)](CH₃OH) (**1**) and [CuHL](CH₃OH) (**2**), where H₃L is *N,N'*-bis(5-methylsalicylidene)-2-hydroxy-1,3-propanediamine. The result of the reactions between 5-methylsalicylaldehyde and 2-hydroxy-1,3-propanediamine in the presence of lanthanide ions and/or copper(II) ion was *N,N'*-bis(5-methylsalicylidene)-2-hydroxy-1,3-propanediamine (H₃L **B**) or [CuHL](CH₃OH) (**2**), respectively. Structures of the compounds were determined by single-crystal X-ray diffraction and physicochemical methods. The microstructures and phase compositions of crystals were studied by scanning electron microscopy (SEM). In dinuclear complex [Cu₂L(CH₃COO)(CH₃OH)](CH₃OH) (**1**), two copper(II) ions are bond to one H₃L ligand and one acetate ion. Coordination modes of the two copper centers are different: the geometry of copper 1 is almost ideal square-planar, while that for copper 2 can be described as tetragonal pyramidal. In complex [CuHL](CH₃OH) (**2**), the copper(II) ion is four coordinated and the coordination, rather than square-planar, can be described as flattened tetrahedral. Formation of complexes between copper(II) or lanthanide ions with *N,N'*-bis(5-methylsalicylidene)-2-hydroxy-1,3-propanediamine (H₃L) was also studied in solution by pH potentiometry. It should be mentioned that the complexes of lanthanide ions exist only in solution. Additionally, the salen-type ligand H₃L and its dinuclear and mononuclear copper(II) complexes were studied by cyclic voltammetry, and their spectroelectrochemical properties were examined.

Received 25th April 2018
 Accepted 18th August 2018

DOI: 10.1039/c8ra03565b

rsc.li/rsc-advances

Introduction

Preparation of flexible Schiff-base salen-type ligands and their complexes with d- and f-electron metal ions is an interesting and important topic due to their broad applications.¹ The combination of properties of such type of ligands with the requirements of metal ions led to novel and unusual mononuclear² and polynuclear³ coordination compounds.

Salen-type ligands attract attention from researchers because of their antitumoral, antibacterial, antiviral and antifungal activities, which can be improved by coordination of ligands to the metal ion.⁴

Transition metal complexes with salen-type ligands have applications in heterogenous and homogenous catalysis,⁵ diagnostic pharmaceuticals and laser technology.⁶ Additional reasons for current interest in salen-type complexes derive from their magnetic⁷ and optical properties.⁸ Copper(II) ion complexes of various Schiff bases and polyamine ligands⁹ are excellent systems for DNA, RNA and phosphodiester hydrolysis. These types of compounds are able to bind and cleave DNA.¹⁰ Design and synthesis of metal complexes with salen-type ligands, particularly polynuclear ligands, are very important in the study of the relationship between the structure and biological functions of complexes.¹¹ Moreover, Schiff-base complexes can play a role of model compounds of naturally occurring metalloenzymes.¹² Potential applications of Schiff base complexes, particularly biological¹³ and diagnostic¹⁴ activities, encouraged us to continue our studies of these complexes.

Salen-type ligands are generally tetradentate with an N₂O₂ set of donor atoms. They are constructed from derivatives of salicylaldehyde and various diamines and are obtained from condensation reactions.¹⁵ In this paper, the tetradentate donor atom

Faculty of Chemistry, Adam Mickiewicz University, Umultowska 89b, 61-614 Poznań, Poland. E-mail: gosiati@amu.edu.pl; Tel: +48 61829 1553

† Electronic supplementary information (ESI) available: Spectroelectrochemistry and potentiometric data, the difference Fourier maps. CCDC 1569983 (H₃L A), 1569984 (H₃L B), 1569985 (**1**), and 1569986(**2**). For ESI and crystallographic data in CIF or other electronic format see DOI: 10.1039/c8ra03565b



system was modified by the use of 2-hydroxy-1,3-propanediamine. The new ligand *N,N'*-bis(5-methylsalicylidene)-2-hydroxy-1,3-propanediamine (H_3L , Fig. 1) with an N_2O_3 set of donor atoms and its resulting complexes have been obtained. The use of this spacer between the two salicylic moieties was dictated by the coordination requirements of lanthanide ions, which exhibit high coordination numbers and flexible coordination environments.¹⁶ The new flexible ligand *N,N'*-bis(5-methylsalicylidene)-2-hydroxy-1,3-propanediamine (H_3L) is a good candidate to form novel 3d, 4f and 3d–4f architectures. We report the preparation and crystal structures of new Schiff-base complexes with copper(II), dysprosium(III) and terbium(III) ions. Moreover, the stability constants of the complexes formed in reactions between *N,N'*-bis(5-methylsalicylidene)-2-hydroxy-1,3-propanediamine (H_3L , Fig. 1) and Cu(II), Dy(III), and Tb(III) ions in water were determined by potentiometric titration in water solution.

Thus far, potentiometric studies of salen-type ligands, due to insolubility of such type of ligands in water, have been performed in mixtures of organic solvents (dimethyl sulfoxide, methanol, ethanol, dioxane, or dimethyl sulfoxide) with water. Additionally, spectroelectrochemical properties of dinuclear and mononuclear copper(II) complexes with salen-type ligands have not been widely examined.

Microstructures and phase compositions of crystals were studied by scanning electron microscopy (SEM).

Results and discussion

The studied compounds were obtained in template reactions of 5-methylsalicylaldehyde and 2-hydroxy-1,3-propanediamine in the presence of copper(II) acetate or appropriate lanthanide(III) nitrate. Heteronuclear compounds were also obtained in template reactions of 5-methylsalicylaldehyde and 2-hydroxy-1,3-propanediamine in the presence of copper(II) acetate and appropriate lanthanide(III) nitrate, as shown in Scheme 1.

Condensation reaction between 5-methylsalicylaldehyde and 2-hydroxy-1,3-propanediamine led to formation of the ligand H_3L **A**, whereas the ligand H_3L **B** was obtained in the template condensation reaction between 5-methylsalicylaldehyde and 2-hydroxy-1,3-propanediamine in the presence of selected lanthanide(III) ions. Template condensation reactions of 5-methylsalicylaldehyde and 2-hydroxy-1,3-propanediamine in the presence of copper(II) acetate and Ln(III) nitrates (Ln = Tb(III), Dy(III)) led to the formation of mononuclear complexes containing only copper(II) ion $[CuHL](CH_3OH)$ (2). Moreover, in the condensation reaction between 5-methylsalicylaldehyde and 2-hydroxy-1,3-propanediamine in the presence of two equivalents of copper(II) ions, the dinuclear complex $[Cu_2L(CH_3COO)(CH_3OH)](CH_3OH)$ (1) was obtained.

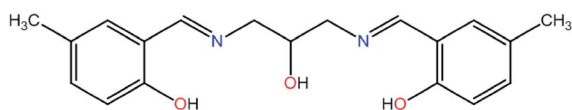


Fig. 1 Formula of *N,N'*-bis(5-methylsalicylidene)-2-hydroxy-1,3-propanediamine (H_3L).

Compositions of resulting complexes were defined using single-crystal X-ray diffraction analysis, microanalysis (CHN), IR, ESI-MS, 1H and ^{13}C NMR spectroscopy, and scanning electron microscopy (SEM). For all compounds, electrochemical and spectroelectrochemical measurements were recorded.

The ligand H_3L was found in two different crystalline forms: polymorphs **A** and **B**. In both forms, the molecule is essentially non-symmetric. The difference Fourier maps (Fig. S1–S4†) as well as successful refinement of hydrogen atoms show that hydrogen atoms are bonded to an oxygen atom on one side of the molecule and to a nitrogen atom on the other side (Fig. 2). This is additionally confirmed by the significant differences in the C–N–C bond angles (Table 1), which are connected with the presence/absence of a bonded hydrogen atom.

Conformations of the molecules are quite different. Fig. 3 shows a comparison of the two molecules and Table 1 contains selected torsion angles. It might be noted that the orientation of O1 hydroxyl group is also different: N–C–C–O torsion angles are $-163.85(18)^\circ$ and $55.2(2)^\circ$ in H_3L **A**, while in H_3L **B** these values are $-68.4(5)^\circ$ and $71.7(5)^\circ$. In addition, the supramolecular motifs in the two crystal structures are essentially different. In both cases the main driving force is O1...O15 intermolecular hydrogen bonding. In non-centrosymmetric (space group *Pc*) H_3L **A**, these bonds connect molecules into infinite chains (Fig. 4a), but in centrosymmetric (*Pccn*) H_3L **B**, the molecules form hydrogen-bonded dimers (Fig. 4b). This can be correlated with the quality of crystals: chains generally need more time and exhibit slower crystal formation than dimers.

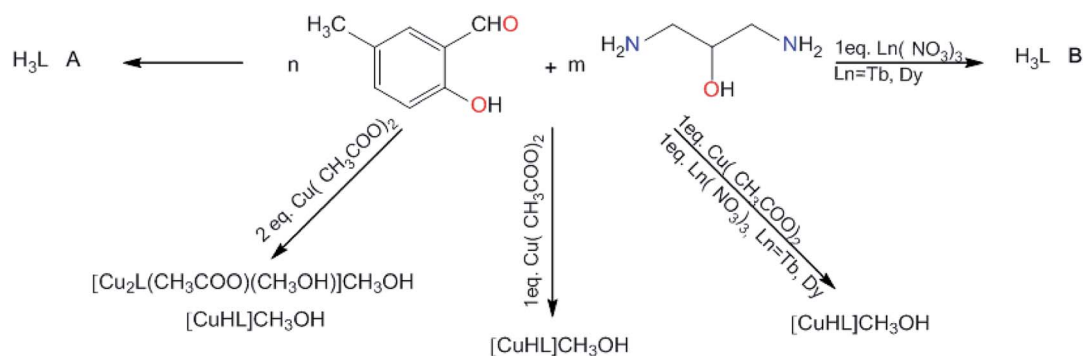
Interestingly, the ligand makes two forms of complexes with copper. In two-centered complex $[Cu_2L(CH_3COO)(CH_3OH)](CH_3OH)$ (1), two symmetry-independent Cu ions are bonded to one ligand molecule (Fig. 5) and one acetate ion. The central O1 atom is coordinated to two copper centers. However, the coordination modes of the two Cu centers are different: for Cu1 the coordination number is 4 (O₂N from ligand, additional oxygen atom from coordinated acetate ion) and the geometry around Cu1 is almost ideally square-planar (*cf.* Table 1); Cu2 is 4 + 1 coordinated, with four atoms similar to Cu1 (O₃N) and an additional oxygen atom with longer Cu–O distance.

This can be described as tetragonal pyramid, with Cu ion displaced from the base plane towards the apex oxygen atom by 0.121(1) Å. The crystal structure additionally contains a methanol (solvent) molecule, which is involved in the hydrogen-bonding system that connects molecules into a three dimensional network.

Complex $[CuHL](CH_3OH)$ (2) is one-centered: the Cu(II) ion is four coordinated by two nitrogen and two oxygen atoms from the ligand molecule (Fig. 6). The coordination is far from square-planar; rather, it can be described as considerably flattened tetrahedral (*cf.* Table 1). Such different coordination modes are possible because of the flexibility of the ligand (Fig. S5,† Table 1).

The molecules in complex (2) are joined into infinite chains by means of O–H...O hydrogen bonds (Fig. 7, Table 2). Interestingly, the OH group is disordered between two positions, with two different orientations around C1 atom (Table 1), and





Scheme 1 Synthetic routes of preparation of complexes (1), (2), and ligands H₃L A and H₃L B, where $n = 1, 2$ or 8 ; $m = 1, 2$ or 3 .

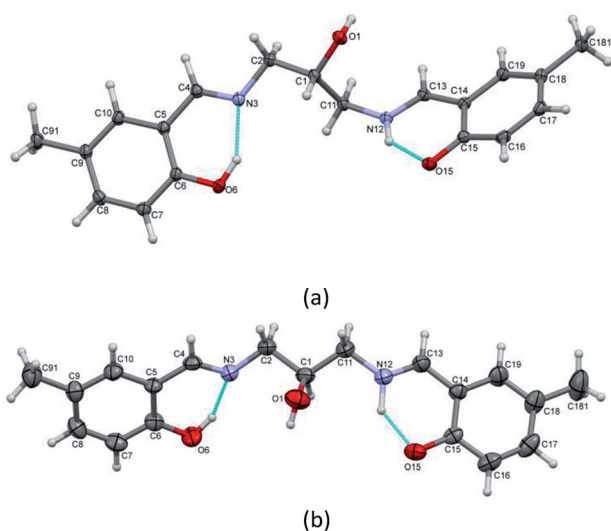


Fig. 2 Perspective views of two forms of ligand molecule (a) H₃L A and (b) H₃L B with numbering scheme. Ellipsoids are drawn at 50% probability level, hydrogen atoms are represented by spheres of arbitrary radii and intramolecular hydrogen bonds are drawn as dashed lines.

the alternative positions are hydrogen-bonded to two different oxygen atoms of the neighbouring molecule.

Photophysical properties

IR spectroscopy. Important features of the IR spectra of ligand H₃L and its complexes include the appearance of vibration at 1632–1624 cm⁻¹ for these compounds. These bands and the absence of characteristic aldehyde and amine bands of the starting materials confirm the formation of the Schiff-base (C=N) groups.²⁴ The shift of the bands to 1630–1624 cm⁻¹ for complexes compared to the free ligand (1632 cm⁻¹) shows that metal ions are coordinated to nitrogen atoms of imino groups.²⁵ The bands at 1279 cm⁻¹ for ligand H₃L and in the range of 1165–1160 cm⁻¹ for the complexes are assigned to vibrations of the C–O group; location of the bands for the complexes suggests the involvement of phenolic oxygen in the metal–ligand coordination.²⁶ The band at 3389–3163 cm⁻¹ in the IR spectrum of the complex corresponds to the vibration of –OH group from the methanol molecules. The spectrum of H₃L shows an

absorption band at 3277 cm⁻¹ due to the formation of intramolecular hydrogen bonding, while the band at 2917 cm⁻¹ confirms the intermolecular hydrogen bonding that connects the H₃L A and H₃L B molecules into infinite chains and dimers, respectively, which is in good agreement with the crystal structures. Cu–N and Cu–O stretching bands appear at 563–550 cm⁻¹ and 503–496 cm⁻¹, confirming the participation of phenolic oxygens and imine nitrogens, respectively, in the metal–ligand coordination. These bands are absent in the spectrum of the free ligand. The IR spectrum of [Cu₂L(CH₃COO)(CH₃OH)](CH₃OH) (1) complex shows two strong bands at 1564 and 1427 cm⁻¹, which were assigned to the coordinated acetate group. The average difference between 1564 and 1427 cm⁻¹ (137 cm⁻¹) indicates the bridging coordination mode of acetate ion.²⁷

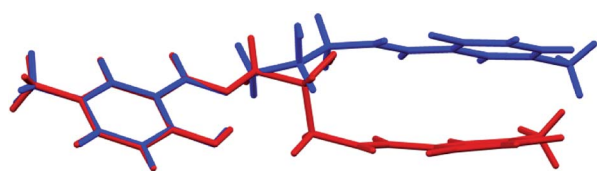
Electrospray mass spectrometry. Experiments were performed in methanol. The ESI spectrogram of [Cu₂L(CH₃COO)(CH₃OH)](CH₃OH) (1) complex showed an intense peak at $m/z = 531.1$, corresponding to the fragment (Cu₂(C₁₉H₁₉N₂O₃)(CH₃COO) + Na)⁺, and a peak of lower intensity at 547.1, assigned to the fragment (Cu₂(C₁₉H₁₉N₂O₃)(CH₃COO) + K)⁺. ESI-MS spectra of all the obtained [CuHL](CH₃OH) (2) complexes showed peaks for fragments (Cu₂(C₁₉H₂₀N₂O₃)₂ + Na)⁺ and (Cu(C₁₉H₂₀N₂O₃) + Na)⁺ at 797.0 and 410.2, respectively. Spectrum of H₃L contains peaks at $m/z = 327.3$ (C₁₉H₂₂N₂O₃ + H)⁺ and $m/z = 325.3$ (C₁₉H₂₁N₂O₃)⁻, which correspond to the mass of the ligand. The conversion to ionic form caused the ESI-MS study to show the additional proton, leading to (C₁₉H₂₂N₂O₃ + H)⁺. Alternatively, the addition of sodium or potassium ion led to the formation of (Cu₂(C₁₉H₁₉N₂O₃)(CH₃COO) + K)⁺ or (Cu(C₁₉H₂₀N₂O₃) + Na)⁺. The characteristic molecular peaks for the complexes and ligand (H₃L) in the mass spectrum are in good agreement with the molecular formulae postulated for the complexes and the ligand.

NMR spectroscopy. ¹H NMR spectroscopy of H₃L in DMSO-*d*₆ solution shows a characteristic signal at δ 8.46 ppm, attributed to protons of imine groups, which confirms the condensation reaction of two 5-methylsalicylaldehyde molecules with one 2-hydroxy-1,3-propanediamine molecule. The signal at δ 13.22 ppm corresponds to –OH protons of benzylidene rings, while the signal at δ 13.22 ppm corresponds to –OH protons from a polyamine chain. Signals in the region δ 7.23–6.78 ppm



Table 1 Selected bond lengths (Å) for H₃L A, H₃L B, (1) and (2)

	H ₃ L A	H ₃ L B	1	2
Cu1–O1			1.9014(15)	Cu1–N3 1.9431(18)
Cu1–O6			1.9078(16)	Cu1–O6 1.9086(15)
Cu1–N3			1.9283(19)	Cu1–N12 1.9434(18)
Cu1–O1B			1.9379(16)	Cu1–O15 1.9055(15)
Cu2–O1			1.9248(15)	
Cu2–O15			1.9048(16)	
Cu2–N12			1.950(2)	
Cu2–O2B			1.9649(16)	
Cu2–O1D			2.488(2)	
C1–O1	1.422(3)	1.426(5)	1.437(3)	1.424(4)
				1.433(3)
C2–N3	1.460(3)	1.440(5)	1.473(3)	1.469(3)
N3–C4	1.275(3)	1.271(5)	1.283(3)	1.284(3)
C6–O6	1.353(7)	1.338(5)	1.323(3)	1.319(3)
C11–N12	1.455(3)	1.449(5)	1.472(3)	1.469(3)
N12–C13	1.299(3)	1.273(5)	1.280(3)	1.282(3)
C15–O15	1.287(3)	1.320(5)	1.315(3)	1.317(3)
2 largest			174.67(7)	153.31(8)
			179.54(8)	153.18(8)
			177.42(7)	
			166.94(8)	
C2–N3–C4	118.33(19)	119.0(4)	121.1(2)	119.74(19)
C11–N12–C13	122.81(19)	122.7(4)	120.9(2)	119.73(18)
C6–C5–C4–N3	2.6(3)	2.3(7)	2.5(4)	5.4(4)
C5–C4–N3–C2	−179.39(19)	177.8(4)	−173.7(2)	−179.8(2)
C4–N3–C2–C1	168.6(2)	137.7(5)	−150.5(2)	−113.9(2)
N3–C2–C1–O1	−163.85(18)	−68.4(5)	−35.3(3)	83.8(2)
				−153.5(2)
N3–C2–C1–C11	71.8(2)	175.8(4)	−156.2(2)	−37.5(3)
C2–C1–C11–N12	179.10(17)	−170.1(4)	164.0(2)	−35.1(3)
O1–C1–C11–N12	55.2(2)	71.7(5)	42.4(3)	−153.5(2)
				85.7(3)
C1–C11–N12–C13	−93.5(3)	148.9(4)	158.6(2)	−115.6(2)
C11–N12–C13–C14	167.8(2)	−178.1(4)	178.6(2)	−178.6(2)
N12–C13–C14–C15	−5.5(3)	2.9(7)	−0.5(4)	6.1(4)
A/B	42.36(7)	49.89(17)	21.15(7)	48.83(8)

Fig. 3 Comparison of conformations of H₃L A and B molecules' crystalline forms.

are assigned to protons of benzylidene ring groups. Singlets at δ 3.75 and δ 2.24 ppm correspond to protons of methylene and methyl groups, respectively. The ¹³C NMR spectrum of H₃L in DMSO-*d*₆ shows sharp signals corresponding to carbon atoms in the proposed structure. The signal observed at δ 159.88 is assigned to azomethine carbon atoms. The resonance signals for aromatic carbon atoms appeared at δ 166.4 ppm and in the range of δ 133.42–117.70 ppm. The signal observed at δ 69.89 ppm corresponds to carbon of the CH(OH)– group. Sharp signals corresponding to methylene and methyl carbon atoms are observed at δ 63.38 and 20.39 ppm, respectively.

Scanning electron microscopy (SEM)

To investigate the microstructure and measure the composition of obtained crystals, scanning electron microscopy (SEM) was used. As shown in Fig. 8, the crystals have cubic and oblong shapes. Their sizes range from 5 to 15 μ m. However, smaller fragments of crystals are also observed. SEM analysis confirms the data acquired from crystallographic measurements: the cubic crystals are dinuclear complex [Cu₂L(CH₃COO)(CH₃–OH)](CH₃OH) (1) and the needle-like crystals are mononuclear [CuHL](CH₃OH) (2). Moreover, needle-like crystals occur on the surface of cubic crystals, as visible in Fig. 8a.

Potentiometric measurements

The formation of complexes between *N,N'*-bis(5-methylsalicylidene)-2-hydroxy-1,3-propanediamine (H₃L) and Cu²⁺, Tb³⁺ and Dy³⁺ ions was studied by potentiometry titration. Potentiometric titration was performed in water (p*K*_w = 13.86). On the basis of computer analysis of the potentiometric data (HYPERQUAD program), the three protonation constants of *N,N'*-bis(5-methylsalicylidene)-2-hydroxy-1,3-propanediamine



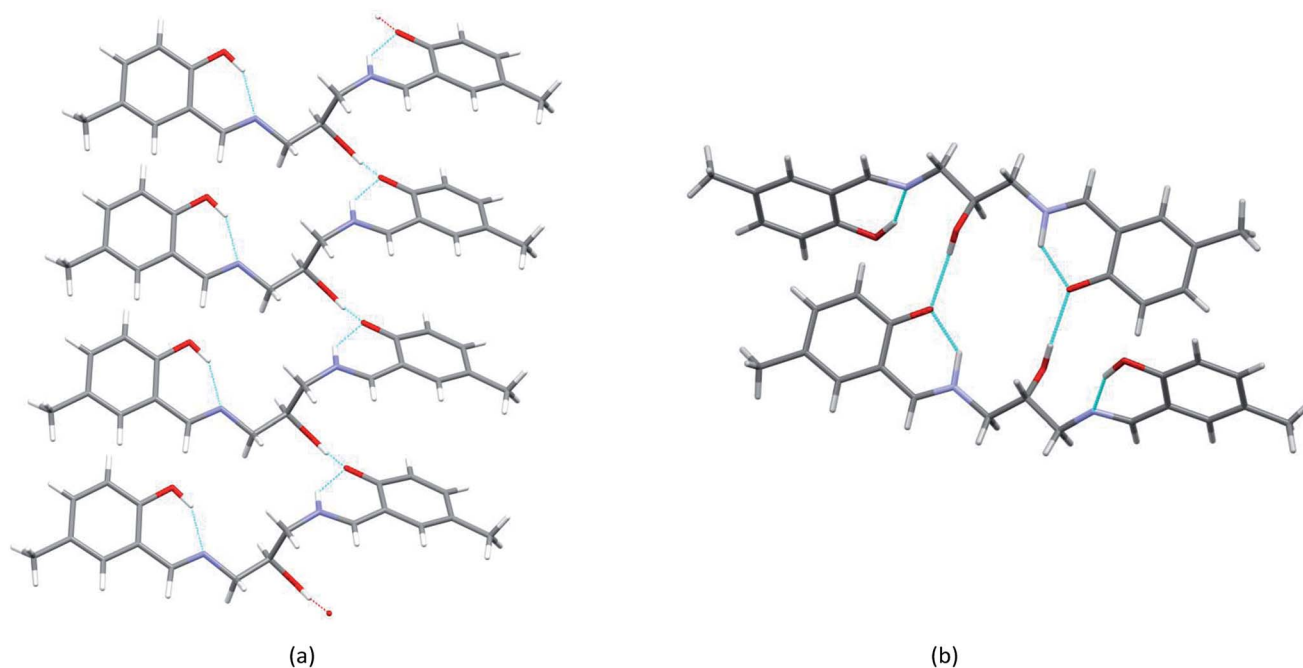


Fig. 4 Supramolecular hydrogen-bond motifs created by H_3L molecules in two polymorphic forms: (a) chains in H_3L A and (b) dimers in H_3L B.

(H_3L) were determined: $\log K_1 = 22.07$, $\log K_2 = 8.77$ and $\log K_3 = 8.23$. The structural formula of the ligand studied is presented in Fig. 1. N,N' -bis(5-methylsalicylidene)-2-hydroxy-1,3-propanediamine exists in solution in protonated form (H_3L) and partially (H_2L^- and HL^{2-}) and fully (L^{3-}) deprotonated forms.

Distribution diagram for H_3L ligand shows that in the pH range 2.5–8.0, the fully protonated form H_3L dominates, but at pH 8.5, the three forms H_3L , H_2L^- and HL^{2-} coexist, and above 9.0, HL^{2-} dominates (Fig. 9). Successive values of $\log K_1 = 8.23$ and $\log K_2 = 8.77$ correspond to the protonation of phenolic groups, whereas $\log K_3 = 22.07$ corresponds to the protonation of an imine nitrogen.²⁸

The overall stability constants ($\log \beta$) and equilibrium constants ($\log K$) of the complexes formed in the Cu/H_3L and Ln/H_3L ($Ln = Tb^{3+}$ and Dy^{3+}) systems are listed in Tables 3–5. For the sake of simplicity, ion charges in potentiometric descriptions of the complexes were omitted. Hydrolysis constants for metal ions were taken into account. The assumed

model was verified by analysis of the standard deviations, convergence of the experimental data and the theoretical curve obtained for the chosen model (evaluated by Hamiltonian and chi squared tests, Fig. S6†).

Computer analysis of the potentiometric titration data for the Cu^{2+}/H_3L system confirmed the formation of $CuHL$, CuL , $CuL(OH)$ and Cu_2L complexes. The formation of Cu_2L was found only for copper(II) ion system Cu^{2+}/H_3L with 2 : 1 molar

Table 2 Hydrogen bond data (\AA , $^\circ$) with s.u.'s in parentheses^a

D	H	A	D–H	H \cdots A	D \cdots A	D–H \cdots A
H_3L A						
O10	H1O	O15 ⁱ	1.00(4)	1.67(4)	2.671(2)	174(4)
O6	H6	N3	0.91(4)	1.78(4)	2.593(3)	148(4)
N12	H12	O15	0.91(4)	1.84(4)	2.617(3)	142(3)
H_3L B						
O1	H1O	O15 ⁱⁱ	0.82	1.92	2.718(4)	165
O6	H6	N3	0.90(5)	1.74(5)	2.580(5)	153(4)
N12	H12	O15	1.05(6)	1.66(6)	2.534(5)	137(4)
1						
O1C	H1C	O6A ⁱⁱⁱ	0.84	1.96	2.793(2)	175
O1D	H1D	O1C	0.84	1.91	2.738(3)	171
2						
O1	H1B	O6 ^{iv}	0.84	1.86	2.694(3)	171
O1'	H10	O15 ^{iv}	0.84	1.83	2.652(4)	167
O1A	H1A	O1 ^v	0.84	2.00	2.697(7)	140
C3	H3	O13	1.00	2.29	3.0590(19)	133

^a Symmetry codes: ⁱ $x, -1 + y, z$; ⁱⁱ $1 - x, 1 - y, 1 - z$; ⁱⁱⁱ $1/2 - x, 1/2 + y, 3/2 - z$; ^{iv} $x, 1/2 - y, 1/2 + z$; ^v $x, 1/2 - y, -1/2 + z$.

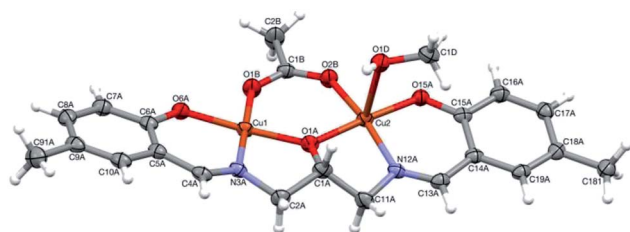


Fig. 5 Perspective view of **1** with numbering scheme. Ellipsoids are drawn at 50% probability level and hydrogen atoms are represented by spheres of arbitrary radii.



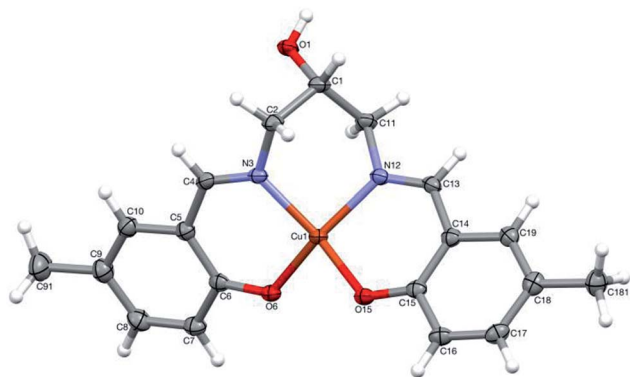


Fig. 6 Perspective view of **2** with numbering scheme. Ellipsoids are drawn at 50% probability level and hydrogen atoms are represented by spheres of arbitrary radii.

ratio. The concentration of complex CuHL is extremely low and the coordination type is impossible to determine. Cu₂L complex starts to form in solution at about pH 6.5 and dominates at about pH 8.0, bonding about 65% of the metal ion in the solution. The hydroxocomplex CuL(OH) starts to form at about pH 7.5 and dominates above pH 9.5 (Fig. 10).

For Ln/H₃L systems, where Ln = Tb³⁺ and Dy³⁺ with molar ratios 1 : 1 and 1 : 2, the formation of the following complexes LnHL, LnL, and LnL(OH) and Ln(H₂L)₂, Ln(HL)₂ and Ln(HL)L respectively.

The complexes LnHL, LnL and LnL(OH) (where Ln = Tb³⁺ and Dy³⁺) start forming in solution at about pH 7.0 and dominate at pH close to 8.0 and 9.0, respectively. However, complex LnL(OH) starts to form at pH 7 and dominates in pH range 7.0–11.0. Complexes Ln(H₂L)₂ and Ln(HL)L form in systems with molar ratio Ln : H₃L = 1 : 2. They start to form at pH 6. Complex Ln(H₂L)₂ dominates at pH 8 for dysprosium(III) and at pH 9.0 for terbium(III), while complex Ln(HL)L dominates in pH range of 7.0–11.0 (Fig. 11). It is worth noting that the complexes of Tb(III) and Dy(III) ions with H₃L ligand formed only in solution and their compositions depend on the molar ratio of the starting materials.

Electrochemical studies

Cyclic voltammetry and spectroelectrochemical studies of the Schiff-base ligand H₃L and its dinuclear and mononuclear copper(II) complexes were conducted to determine the influence of nuclearity and coordination geometry on the change in Cu(II/I) reduction and oxidation potentials upon coordination of the ligand to copper(II) ions as well as their electrochromical properties. Measurements were recorded in acetonitrile solution with 0.1 M tetrabutylammonium hexafluorophosphate (TBAPF₆) as the supporting electrolyte. Fig. 12 shows cyclic voltammograms of free ligand H₃L and Cu(II) complexes dinuclear [Cu₂L(CH₃COO)(CH₃OH)](CH₃OH) (**1**) and mononuclear [CuHL](CH₃OH) (**2**).

Free ligand H₃L scanned in the negative direction undergoes irreversible reduction at $E_{pc} = -300$ mV and irreversible oxidation at $E_{pa} = +1030$ mV. Fig. 13 shows the spectroelectrochemical behaviour of free ligand H₃L.

Within the UV spectrum of the ligand H₃L, the existence of one absorption band assigned to the $\pi-\pi^*$ transition²⁹ at 315 nm was observed. When stepwise negative potential was applied, gradual decrease of this band was observed, which was concomitant with the formation of a new band at 390 nm. The sharp isosbestic point at 345 nm confirms the presence of only two independent species in solution: neutral and reduced. The original spectrum of H₃L ligand was obtained by applying positive potential of +700 mV. The visible color change during reduction was from colorless to yellow. Dinuclear complex (**1**) showed irreversible electrochemical behaviour with two reduction potentials at $E_{pc} = -600$ mV and -910 mV and three irreversible oxidation potentials at $E_{pa} = +610$ mV, $+1060$ mV, and $+1210$ mV. The first reduction potential is assigned to Cu(II)/Cu(I) \rightarrow Cu(II)/Cu(I), while the second reduction potential is assigned to the reduction of Cu(II)/Cu(I) \rightarrow Cu(I)/Cu(I), which is probably concomitant with the H₃L \rightarrow H₂L⁻ reduction process. To verify assignment of the reduction waves, spectroelectrochemical measurements were recorded (Fig. 14).

Dinuclear Cu(II) complex [Cu₂L(CH₃COO)(CH₃OH)](CH₃OH) (**1**) in its neutral state exhibited two absorption bands: one at

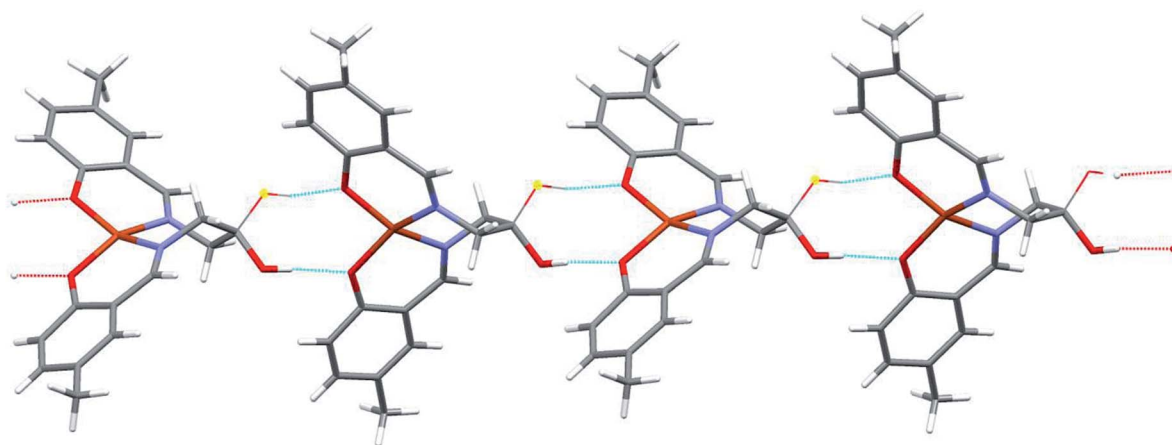
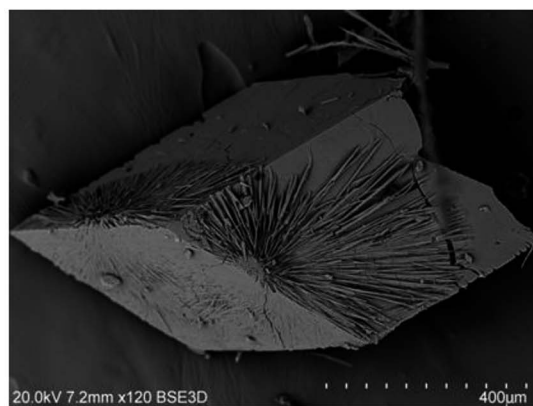
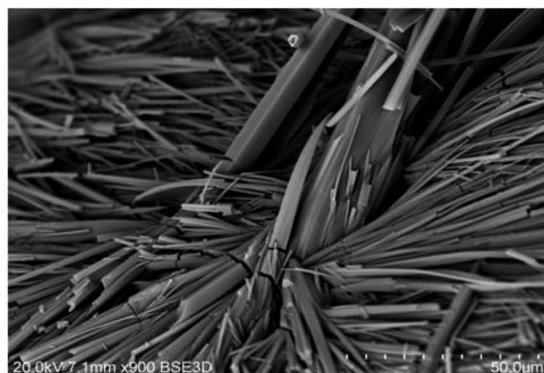


Fig. 7 Hydrogen-bonded chain of complex molecules **2**. Thin lines show the alternative positions of OH groups (*cf.* text).





(a)



(b)

Fig. 8 SEM micrographs (BSE mode) of sample (1) at different magnifications.

378 nm, which is ligand-based absorption, and a second at 630 nm, which is assigned to d-d transition.³⁰ When negative potential in the range from -100 mV to -600 mV was applied, a decrease in the d-d transition band and no change in the ligand-based absorption band were observed. Further decrease in the reduction potential causes disappearance of the d-

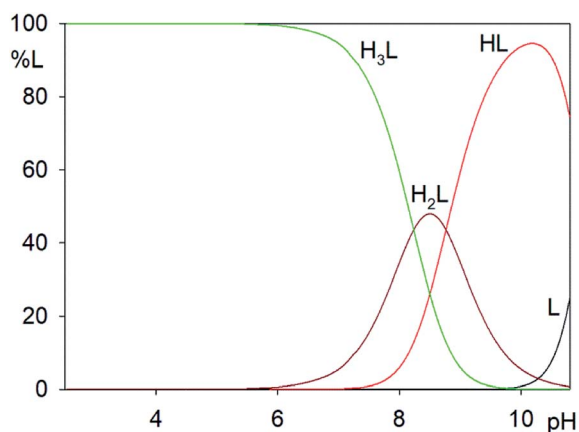


Fig. 9 Distribution diagrams for *N,N'*-bis(5-methylsalicylidene)-2-hydroxy-1,3-propanediamine (H_3L), c $H_3L = 0.002$ M. Percent of species refers to relative concentration of ligand.

d transition band and shift in the ligand-based band to 555 nm. During this process, the colour of the solution changed from green to yellow. The oxidation of complex (1) leads to three irreversible processes. The first at $+610$ nm is the $Cu(I)/Cu(I) \rightarrow Cu(II)/Cu(I)$ oxidation process, while the second at $+1060$ mV is probably assigned to the $Cu(II)/Cu(I) \rightarrow Cu(II)/Cu(II)$ process. The ligand-based oxidation process was observed at $+1210$ mV and is shifted to a more positive value, by 180 mV, in comparison to the free ligand, which is the consequence of stabilization of the ligand molecule in transition metal complexes.³¹ All mononuclear complexes exhibit the same electrochemical behaviour (Fig. 12 and S7[†]). In the cyclic voltammogram of complex (1), one irreversible cathodic peak at -410 mV was observed, which is assigned to the $Cu(II) \rightarrow Cu(I)$ reduction process, concomitant with the reduction of the ligand molecule. Spectral changes during reduction of mononuclear complexes were similar to those observed for complex (2) at the second reduction state (Fig. 15, S8 and S9[†]).

Experimental

Materials

Copper(II) acetate anhydrous, terbium(III) nitrate pentahydrate, dysprosium(III) nitrate hexahydrate, 5-methylsalicylaldehyde and 2-hydroxy-1,3-propanediamine were purchased from Aldrich Chemical Company and used without further purification.

Physical measurements

Mass spectra were performed using electrospray ionization (ESI) techniques. Electrospray mass spectra were determined in methanol using Waters Micromass ZQ spectrometer. Samples were run in positive-ion mode. Concentration of the compound was about 10^{-4} mol dm^{-3} . Scanning was performed from $m/z = 100$ to 1000 in 6 s and 10 scans were averaged to obtain the final spectrum. NMR spectra were recorded in $DMSO-d_6$ on a Bruker Ultrashield 300 MHz spectrometer calibrated against residual protonated solvent signals ($DMSO-d_6$, δ 2.50) given in parts per million. IR spectra were obtained using a FT-IR Nicolet IS 50 spectrometer and peak positions are reported in cm^{-1} . Microanalyses (CHN) were obtained using Elementar Analyser Vario EL III.

X-ray crystallography

X-ray diffraction data were collected by the ω -scan technique on two Rigaku four-circle diffractometers for H_3L A and $[CuHL](CH_3OH)$ (2) at 130(1) K on SuperNova (Atlas detector) with mirror-monochromated CuK_α radiation ($\lambda = 1.54178$ Å), for H_3L B at room temperature, and for $[Cu_2L(CH_3COO)(CH_3OH)](CH_3OH)$ (1) on Xcalibur (Eos detector) diffractometer with graphite-monochromatized MoK_α radiation ($\lambda = 0.71073$ Å). Data were corrected for Lorentz-polarization and absorption effects.¹⁷ Accurate unit-cell parameters were determined by a least-squares fit of 1792 H_3L A, 948 H_3L B, 3602 $[Cu_2L(CH_3COO)(CH_3OH)](CH_3OH)$ (1), and 13 463 $[CuHL](CH_3OH)$ (2) reflections of highest intensity, chosen from the entire



Table 3 Successive protonation constants of H₃L ligand and stability (log β) and equilibrium constants (log K_e) of complexes formed in Cu²⁺/H₃L systems (standard deviations of stability constants given in brackets)

Species ^a	Overall protonation constants log β	Reactions	Successive protonation constants log K ₁₋₃
HL	22.07(5)	L + H ⁺ ⇌ HL	22.07
H ₂ L	30.84(6)	HL + H ⁺ ⇌ H ₂ L	8.23
H ₃ L	39.07(6)	H ₂ L + H ⁺ ⇌ H ₃ L	8.77

Species	Overall stability constants log β	Reactions	Equilibrium constants log K _e
CuHL	24.71(3)	Cu ²⁺ + HL ⇌ CuHL	2.79
CuL	18.55(1)	Cu ²⁺ + L ⇌ CuL	18.55
CuL(OH)	10.15(6)	CuL + H ₂ O ⇌ CuL(OH) + H ⁺	5.86
Cu ₂ L	22.76(2)	CuL + Cu ²⁺ ⇌ Cu ₂ L	4.21

^a For the sake of clarity, the charges of individual species have been omitted.

experiment. Structures were solved with SHELXT and refined with the full-matrix least-squares procedure on F² by SHELXL-2014/7.¹⁸ All non-hydrogen atoms were refined anisotropically. NH and OH hydrogen atoms in H₃L were located in the difference Fourier map and isotropically refined. All other hydrogen atoms were placed in the calculated positions and refined using 'riding model' with the isotropic displacement parameters set at 1.2 (1.5 for methyl groups) times the U_{eq} value for appropriate non-hydrogen atoms. In the structure of [CuHL](CH₃OH) (2), disorder was detected: the ligand –OH group was found in two alternative positions, with s.o.f.'s of 57.9(5)/42.1(5)%, and the solvent (methanol) –OH groups are disordered with s.o.f.'s fixed at 67/33% on the basis of displacement parameters. In this last case, constraints were applied in the shape of thermal ellipsoids of disordered atoms. Relevant crystal data and refinement details are listed in Table 6.

Potentiometric measurements

All experimental solutions were prepared using demineralised CO₂-free water. Concentrations of copper(II), terbium(III) and dysprosium(III) ions were determined by inductively coupled plasma optical emission spectrometry (ICP OES). Potentiometric titrations were conducted using Titrand 905 Metrohm

equipped with an autoburette with an i-electrode Metrohm 6.0280.300 calibrated in terms of hydrogen ion concentration prior to each titration.¹⁹

A correction of pH-meter reading was made prior to each measurement series and two standard buffers were used (pH 4.002 and pH 9.225). All potentiometric titrations were made in an atmosphere of neutral gas (helium 5.0) at a constant ionic strength (0.1 M KNO₃) at 20 ± 1 °C using CO₂-free 0.1892 M NaOH as a titrant. Potentiometric titrations were performed for metal : ligand ratios of 1 : 1, 1 : 2 and 2 : 1 for copper and 1 : 1 and 1 : 2 for lanthanide ions (Ln = Tb, Dy). Concentration of H₃L in all systems was 0.001 M acidified with HCl. Molar ratio Ln : H₃L = 2 : 1 was not studied due to the tendency of lanthanide ions to achieve high coordination numbers and inadequate number of donor atoms of H₃L ligand. Determined pK_w for water was 13.86.²⁰ The protonation constants of the N,N'-bis(5-methylsalicylidene)-2-hydroxy-1,3-propanediamine (H₃L), the selection of models, as well as the stability constants of the complexes were determined using HYPERQUAD software. The program uses the non-linear method of least squares to minimize the sum (S) of the squares of residuals between the observed quantities (f^{obs}) and those calculated on the basis of the model (f^{calc})

Table 4 Stability constants (log β) of complexes formed in the Tb³⁺/H₃L and Dy³⁺/H₃L (1 : 1 and 1 : 2) systems (standard deviations of stability constants given in parentheses)

Species ^a	Overall stability constants (log β)			
	Tb : H ₃ L 1 : 1	Tb : H ₃ L 1 : 2	Dy : H ₃ L 1 : 1	Dy : H ₃ L 1 : 2
LnHL	18.80(4)		18.51(9)	
LnL	10.41(3)		10.85(2)	
LnL(OH)	0.32(4)		1.39(4)	
Ln(H ₂ L) ₂		54.30(7)		54.77(8)
Ln(HL) ₂		37.48(6)		37.94(6)
Ln(HL)L		28.49(6)		29.36(7)

^a For the sake of clarity, the charges of individual species have been omitted.

Table 5 Equilibrium constants (log K_e) of complexes formed in Tb³⁺/H₃L and Dy³⁺/H₃L (1 : 1 and 1 : 2) systems

Species ^a	Reactions ^a	Equilibrium constants log K _e	
		Tb ³⁺ /H ₃ L	Dy ³⁺ /H ₃ L
LnHL	Ln ³⁺ + HL ⇌ LnHL	3.26	3.55
LnL	Ln ³⁺ + L ⇌ LnL	10.46	10.85
LnL(OH)	LnL + H ₂ O ⇌ LnL(OH) + H ⁺	3.68	4.30
Ln(H ₂ L) ₂	Ln ³⁺ + 2H ₂ L ⇌ Ln(H ₂ L) ₂	10.46	10.63
Ln(HL) ₂	Ln ³⁺ + 2HL ⇌ Ln(HL) ₂	6.64	7.10
Ln(HL)L	Ln ³⁺ + L + HL ⇌ LnL(HL)	6.42	7.29

^a For the sake of clarity, the charges of individual species have been omitted.



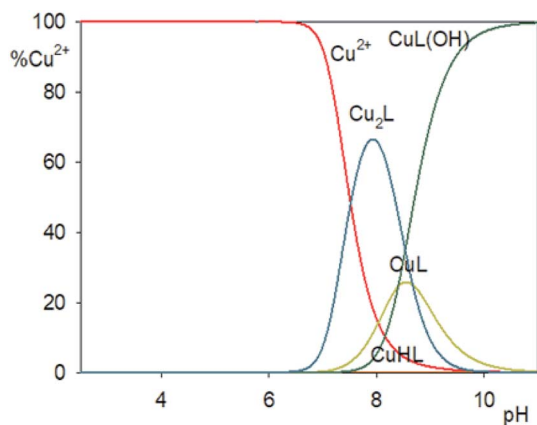


Fig. 10 Distribution diagrams for the $\text{Cu}^{2+}/\text{H}_3\text{L}$ system. Percent of species refers to relative concentration of metal.

$$S = \sum_{i=1}^n w_i (f_i^{\text{obs}} - f_i^{\text{calc}})^2$$

where n = number of measurements and w_i = statistical weight.²¹

Distribution of respective forms was obtained using HySS (Hyperquad Simulation and Speciation) software.²² Calculations were performed using 150–350 points from each titration curve.

In all cases, testing began with the simplest hypothesis and then, in the following steps, the models were expanded to progressively include more species; the results were scrutinized to eliminate the species rejected in the refinement procedures. Criteria used for verification of results were given in an earlier paper.²³

Scanning electron microscope (SEM)

A scanning electron microscope (Hitachi S-3700N) equipped with an electron probe microanalysis system based on energy dispersive X-ray spectroscopy (EPMA-EDXS) managed by Noran SIX system was used to investigate the microstructure and measure phase composition including global composition. For quantitative and qualitative analysis, an acceleration voltage of 20 keV and a working distance of 13.5 mm were used.

Electrochemical studies

Electrochemical and spectroelectrochemical measurements were recorded on a VSP Bio-Logic multichannel potentiostat. Compounds were dissolved in anhydrous and deaerated acetonitrile at $\sim 10^{-4}$ M with 0.1 M tetrabutylammonium hexafluorophosphate as the electrolyte. A platinum electrode was used as the working electrode and a platinum wire was used as the auxiliary electrode. The reference electrode was an Ag/Ag^+ electrode. Spectroelectrochemical measurements were recorded

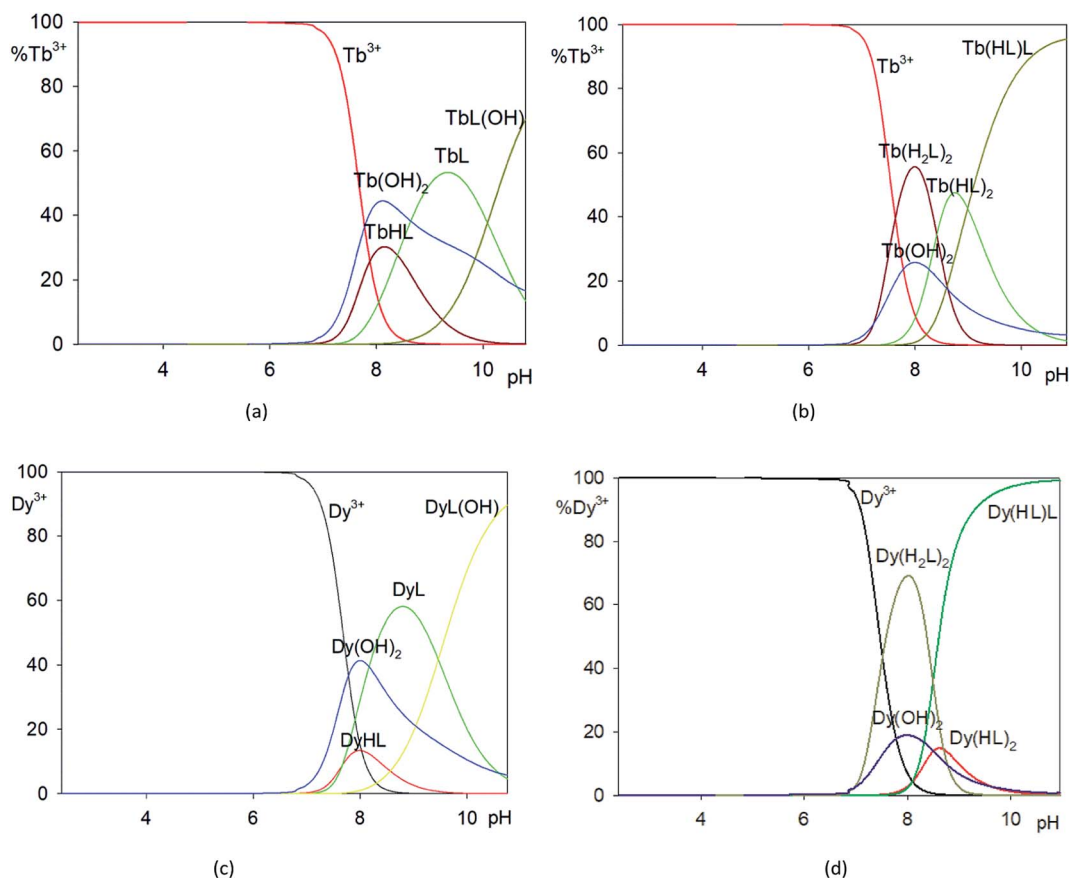


Fig. 11 Distribution diagrams of studied systems: (a) $\text{Tb}^{3+}/\text{H}_3\text{L}$ (1 : 1), (b) $\text{Tb}^{3+}/\text{H}_3\text{L}$ (1 : 2), (c) $\text{Dy}^{3+}/\text{H}_3\text{L}$ (1 : 1), (d) $\text{Dy}^{3+}/\text{H}_3\text{L}$ (1 : 2).



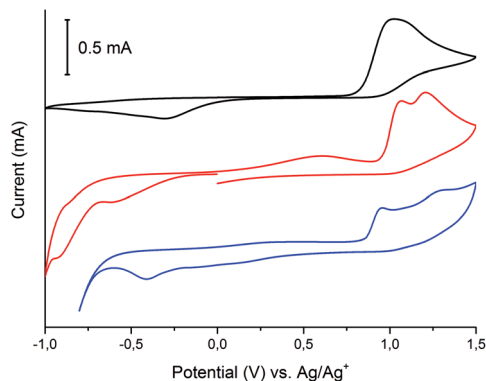


Fig. 12 Cyclic voltammograms of ligand H₃L (black), dinuclear complex (1) (red) and mononuclear complex (2) (blue) measured in anhydrous and deaerated acetonitrile with 0.1 M TBAPF₆ as supporting electrolyte at a scan rate 100 mV s⁻¹ scanned in the negative direction.

using a commercially available platinum honeycomb working electrode on a ceramic support in a narrow optical path quartz cuvette using a miniature Ag/AgCl gel electrode as the reference electrode. Potential was controlled with the potentiostat. The resulting spectroscopic changes were measured with a Jasco V-770 UV-Vis-NIR spectrometer.

Synthesis

Preparation of [Cu₂L(CH₃COO)(CH₃OH)](CH₃OH) (1). To the solution of Cu(CH₃COO)₂ (36 mg, 0.2 mmol) in methanol (10 mL), 5-methylsalicylaldehyde (27.2 mg, 0.2 mmol) in methanol (5 mL) was added and precipitate was formed. Then, 2-hydroxy-1,3-propanediamine (9 mg, 0.1 mmol) in methanol (5 mL) was added dropwise with stirring. The precipitate was dissolved and deep-green solution was obtained. The reaction was conducted for 48 h at room temperature under normal atmosphere. The solution volume was then reduced to 10 mL by roto-evaporation

and then, the solution was kept at low temperature for slow evaporation of solvent. After one week, green cube-like single crystals suitable for X-ray diffraction analysis were formed. The crystals were filtered, washed with cold methanol and dried in air. Green filtrate was left in low temperature for further slow evaporation and after two weeks, green needle-like single crystals suitable for X-ray diffraction analysis were obtained.

[Cu₂L(CH₃COO)](CH₃OH) (1) (green cubes). Yield: 31.8 mg (57.09%). Mp: 224 °C; calculated: C₂₃H₃₀Cu₂N₂O₇ (573.57 g mol⁻¹): C, 48.16; H, 5.27; N, 4.88. Found: C, 48.08; H, 5.22; N, 4.91%. Selected FT-IR (cm⁻¹): 3389 ν(OH), 3011, 2917 ν(OH...N), 1630 ν(C=N), 1160 ν(C-O), 1564, 1427 ν(COO⁻) 558 ν(Cu-O), 496 ν(Cu-N). ESI-MS: *m/z* 531.1 [Cu₂(C₁₉H₁₉N₂O₃)(CH₃COO) + Na]⁺ (100%), 547.1 [Cu₂(C₁₉H₁₉N₂O₃)(CH₃COO) + K]⁺ (40%).

[CuHL](CH₃OH) (2) (green needles). Yield: 32.1 mg (38.67%). Mp: 209 °C; calculated: C₂₁H₂₇CuN₂O₅ (419.56 g mol⁻¹): C, 57.20; H, 5.76; N, 6.67. Found: C, 56.98; H, 5.69; N, 6.74%. ESI-MS: *m/z* 410.2 [Cu(C₁₉H₂₀N₂O₃) + Na]⁺ (100%).

Attempts to synthesize complexes of Ln(NO₃)₃·*n*H₂O, (Ln = Dy, Tb; *n* = 5 or 6) with *N,N*-bis(5-methylsalicylidene)-2-hydroxy-1,3-propanediamine (H₃L): general procedure. To the solution of 5-methylsalicylaldehyde (54.8 mg, 0.8 mmol) in methanol (5 mL), 2-hydroxy-1,3-propanediamine (13.5 mg, 0.3 mmol) in methanol (5 mL) was added dropwise with stirring. Then, triethylamine (42 μL) was added. After 30 min, a solution of appropriate lanthanide(III) nitrate salt (0.1 mmol) in methanol (10 mL) was added and yellow solution was obtained. The reaction was conducted for 48 h at room temperature under normal atmosphere. The solution volume was then reduced to 10 mL by roto-evaporation and the solution was kept at low temperature for slow evaporation of solvent. After two weeks, yellow needle-like crystals suitable for X-ray diffraction analysis were formed. The product was filtered, washed with cold methanol and dried in air.

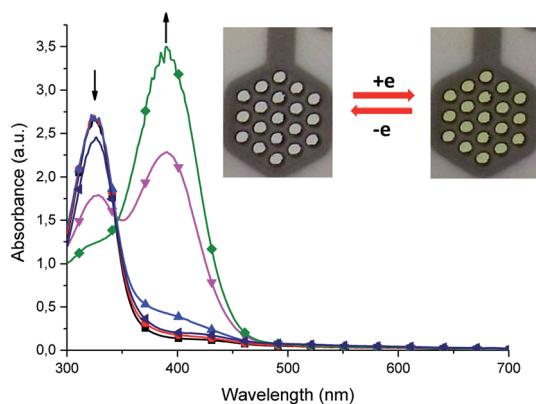


Fig. 13 Spectroelectrochemistry of ligand H₃L in dehydrated and deaerated acetonitrile with 0.1 M TBAPF₆ as the supporting electrolyte by applying 0 (■), -100 (●), -200 (▲), -300 (▼), and -400 mV (◆) followed by +700 mV (◀) potential versus Ag/AgCl gel reference electrode held for 30 s per potential. Inset: photographs of the original H₃L (left) and electrochemically reduced (right) H₃L by applying potential for 30 s.

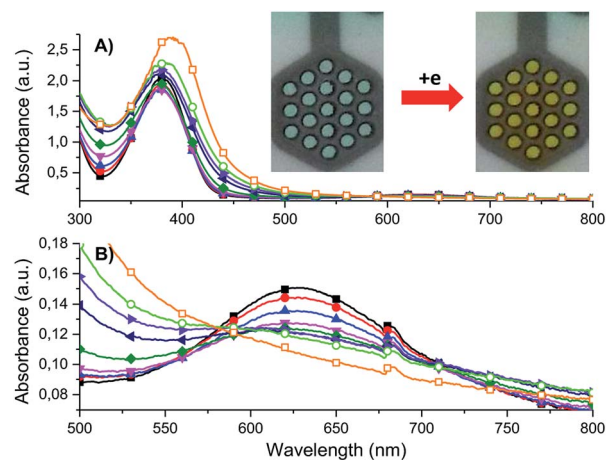


Fig. 14 (A) Spectroelectrochemistry of complex (1) in dehydrated and deaerated acetonitrile with 0.1 M TBAPF₆ as supporting electrolyte by applying 0 (■), -300 (●), -400 (▲), -500 (▼), -600 (◆), -700 (◀), -800 (▶), -900 (○), and -1000 mV (□) potential versus Ag/AgCl gel reference electrode held for 30 s per potential. Inset: photographs of the original H₃L (left) and H₃L electrochemically reduced (right) by applying potential for 30 s. (B) Zoom of 500–800 nm region.



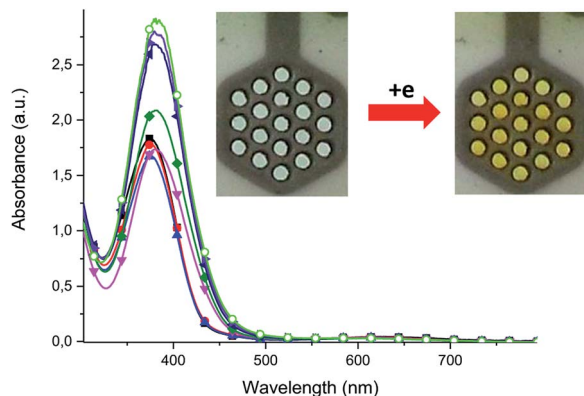


Fig. 15 Spectroelectrochemistry of complex (2) in dehydrated and deaerated acetonitrile with 0.1 M TBAPF₆ as supporting electrolyte by applying 0 (■), -100 (●), -200 (▲), -300 (▼), -400 (◆), -500 (◄), -600 (►), and -700 mV (○) potential versus Ag/AgCl gel reference electrode held for 30 s per potential. Inset: photographs of the original (left) and electrochemically reduced (right) (2) by applying potential for 30 s.

H₃L B yield: 62.46 mg (87.24%). Mp: 160 °C. Calculated: C₁₉H₂₂N₂O₃ (326.38 g mol⁻¹): C, 69.92; H, 6.79; N, 14.71%. Found: C, 69.82; H, 6.72; N, 14.52%. Selected FT-IR (cm⁻¹): 3279 ν(OH), 2914 ν(OH...N), 1632 ν(C=N), 1279 ν(C-O). ¹H NMR (300 MHz, DMSO-*d*₆): δ (ppm): 13.19 (s, 2H; -OH), 8.51 (s, 2H; HC=N), 7.22 (d, *J* = 2.3 Hz, 2H, aromatic), 7.19 (dd, *J* = 8.5 Hz, *JJ* = 2.3 Hz, 2H; aromatic), 6.7 (d, *J* = 8.4 Hz, 2H; aromatic), 5.18 (s, 1H; -OH), 3.76 (dd, *J* = 12.4 Hz, *JJ* = 6.6 Hz, 4H; -CH₂-), 3.61 (dd, *J* = 12.4 Hz, *JJ* = 6.6 Hz, 1H, -CH-), 2.23 (s, 6H; -CH₃). ¹³C NMR (300 MHz, DMSO-*d*₆): δ (ppm): 166.40 (C-OH), 159.88 (HC=N),

133.42 (aromatic), 131.88 (aromatic), 128.21 (aromatic), 119.22 (aromatic), 117.70 (aromatic), 69.89 (-CH(OH)-), 63.38 (-CH₂-), 20.39 (-CH₃). ESI-MS: *m/z* 327.3 [C₁₉H₂₂N₂O₃ + H]⁺ (100%) 325.3, [C₁₉H₂₁N₂O₃]⁻ (100%).

Attempts to synthesize heterodinuclear complexes of Cu(CH₃COO)₂ and Ln(NO₃)₃·*n*H₂O (Ln = Dy, Tb; *n* = 5 or 6) with N,N'-bis(5-methylsalicylidene)-2-hydroxy-1,3-propanediamine (H₃L): general procedure. To the solution of 5-methylsalicylaldehyde (27.2 mg, 0.1 mmol) in methanol (5 mL), 2-hydroxy-1,3-propanediamine (9 mg, 0.2 mmol) in methanol (5 mL) was added dropwise with stirring. After 30 min, a solution of appropriate lanthanide nitrate salt (0.1 mmol) in methanol (5 mL) was added and yellow solution was obtained. After another 30 min, solution of Cu(CH₃COO)₂ (0.1 mmol) in methanol (5 mL) was added and green solution was obtained. The reaction was conducted for 48 h at room temperature under normal atmosphere. The solution was kept at room temperature for slow evaporation of solvent. After one day, green needle-like crystals suitable for X-ray diffraction analysis formed. The product was filtered, washed with cold methanol and dried in air.

The product of the reaction with participation of Tb³⁺ was [CuHL](CH₃OH) (2): yield: 32.10 mg (38.67%). Mp: 210 °C. Calculated: C₂₁H₂₇Cu₂N₂O₅ (419.95 g mol⁻¹): C, 57.20; H, 5.76; N, 6.67. Found: C, 57.11; H, 5.62; N, 6.55%. Selected FT-IR (cm⁻¹): 3163 ν(OH), 2910 ν(OH...N), 1624 ν(C=N), 1165 ν(C-O), 550 ν(Cu-O), 503 ν(Cu-N). ESI-MS: *m/z* 388.2 [Cu(C₁₉H₂₁N₂O₃)H]⁺ (30%), 410.1 [Cu(C₁₉H₂₁N₂O₃)Na]⁺ (100%), 426.1 [Cu(C₁₉H₂₁N₂O₃)K]⁺ (15%).

The product of the reaction with participation of Dy³⁺ was [CuHL](CH₃OH) (2): yield: 28.98 mg (35.46%). Mp: 210 °C.

Table 6 Crystal data and refinement details for H₃L A, H₃L B, (1) and (2)

Compound	H ₃ L A	H ₃ L B	1	2
Formula	C ₁₉ H ₂₉ N ₂ O ₃		C ₂₂ H ₂₆ Cu ₂ N ₂ O ₆ ·CH ₄ O	C ₁₉ H ₂₀ CuN ₂ O ₃ ·CH ₄ O
Formula weight	326.38		573.57	419.95
Crystal system	Monoclinic	Orthorhombic	Monoclinic	Monoclinic
Space group	<i>Pc</i>	<i>Pccn</i>	<i>P2₁/c</i>	<i>P2₁/c</i>
<i>a</i> (Å)	16.4048(13)	9.396(2)	15.4733(4)	11.98914(13)
<i>b</i> (Å)	6.0674(5)	37.076(8)	9.9490(2)	10.38861(9)
<i>c</i> (Å)	8.3490(7)	9.9611(16)	15.8181(6)	16.00151(14)
β (°)	91.077(7)	90	99.548(3)	110.5792(11)
<i>V</i> (Å ³)	830.87(12)	3470.1(12)	2401.37(12)	1865.82(3)
<i>Z</i>	2	8	4	4
<i>d</i> _x (g cm ⁻³)	1.31	1.25	1.59	1.50
<i>F</i> (000)	348	1392	1184	876
μ (mm ⁻¹)	0.717	0.085	1.817	1.896
θ range (°)	2.69–75.24	3.03–25.00	3.32–26.50	5.18–75.61
Reflections				
Collected	2741	13 285	9312	17 812
Unique (<i>R</i> _{int})	2084(0.013)	3049(0.092)	4604(0.020)	3816(0.021)
With <i>I</i> > 2σ(<i>I</i>)	2052	1318	3958	3728
<i>R</i> (<i>F</i>) [<i>I</i> > 2σ(<i>I</i>)]	0.036	0.088	0.030	0.042
w <i>R</i> (<i>F</i> ²) [<i>I</i> > 2σ(<i>I</i>)]	0.096	0.173	0.072	0.118
<i>R</i> (<i>F</i>) [all data]	0.037	0.205	0.038	0.042
w <i>R</i> (<i>F</i> ²) [all data]	0.097	0.214	0.076	0.119
Goodness of fit	1.04	0.98	1.06	1.07
Max/min Δρ (e Å ⁻³)	0.17/−0.17	0.22/−0.21	0.39/−0.40	0.60/−0.54



Calculated: $C_{21}H_{27}Cu_2N_2O_5$ (419.56 g mol⁻¹): C, 57.20; H, 5.76; N, 6.67. Found: C, 57.31; H, 5.80; N, 6.65%. Selected FT-IR (cm⁻¹): 3382 $\nu_{(OH)}$, 2950 $\nu_{(OH...N)}$, 1627 $\nu_{(C=N)}$, 1579, 1466 $\nu_{(C=C)}$, 1162 $\nu_{(C-O)}$, 560 $\nu_{(Cu-O)}$, 501 $\nu_{(Cu-N)}$. ESI-MS: m/z 388.2 $[Cu(C_{19}H_{21}N_2O_3)H]^+$ (100%).

Preparation of $[CuHL](CH_3OH)$ (2). To the solution of $Cu(CH_3COO)_2$ (18 mg, 0.1 mmol) in methanol (10 mL) 5-methylsalicylaldehyde (27.2 mg, 0.2 mmol) in methanol (5 mL) was added and precipitate was formed. Then, 2-hydroxy-1,3-propanediamine (9 mg, 0.1 mmol) in methanol (5 mL) was added dropwise with stirring. The precipitate was dissolved and deep-green solution was obtained. The reaction was performed for 6 h at room temperature under normal atmosphere and green precipitate was formed. The precipitate was filtered, washed with cold methanol and dried in air.

Yield: 37.82 mg (89.62%). Mp: 209 °C. Calculated: $C_{21}H_{27}Cu_2N_2O_5$ (419.95 g mol⁻¹): C, 57.20; H, 5.76; N, 6.67. Found: C, 57.15; H, 5.79; N, 6.70%. Selected FT-IR (cm⁻¹): 3168 $\nu_{(OH)}$, 2921 $\nu_{(OH...N)}$, 1625 $\nu_{(C=N)}$, 1165 $\nu_{(C-O)}$, 563 $\nu_{(Cu-O)}$, 503 $\nu_{(Cu-N)}$. ESI-MS: m/z 410.2 $[Cu(C_{19}H_{20}N_2O_3) + Na]^+$ (100%), 797 $[Cu_2(C_{19}H_{20}N_2O_3)_2 + Na]^+$ (100%).

Synthesis of N,N' -bis(5-methylsalicylidene)-2-hydroxy-1,3-propanediamine - H_3L A. N,N' -Bis(5-methylsalicylidene)-2-hydroxy-1,3-propanediamine (H_3L) was obtained from the condensation reaction of 5-methylsalicylaldehyde (27 mg, 0.2 mmol) and 2-hydroxy-1,3-propanediamine (9 mg, 0.1 mmol). The mixture was stirred in methanol (10 mL) at room temperature for 24 h under normal atmosphere. The resulting yellow solution was left at room temperature for crystallization. Yellow crystals formed after four days. Crystals suitable for X-ray diffraction analysis were collected, washed with cold methanol and dried in air. Yield: 58.46 mg (90.35%). Anal. calcd for $C_{19}H_{22}N_2O_3$ (326.39 g mol⁻¹): C, 69.92; H, 6.79; N, 14.71. Found: C, 69.81; H, 6.81; N, 14.41%. Selected FT-IR (cm⁻¹): 3277 $\nu_{(OH)}$, 2917 $\nu_{(OH...N)}$, 1632 $\nu_{(C=N)}$, 1279 $\nu_{(C-O)}$. ¹H NMR (DMSO-*d*₆): δ (ppm): 13.22 (s, 2H; -OH), 8.46 (s, 2H; HC=N), 7.23 (d, J = 2.2 Hz, 2H, aromatic), 7.14 (dd, J = 8.4 Hz, JJ = 2.2 Hz, 2H; aromatic), 6.78 (d, J = 8.3 Hz, 2H; aromatic), 5.19 (s, 1H; -OH), 3.75 (dd, J = 12.5 Hz, JJ = 6.5 Hz, 4H; -CH₂-), 3.59 (dd, J = 12.5 Hz, JJ = 6.6 Hz, 1H, -CH-), 2.24 (s, 6H; -CH₃). ¹³C NMR (DMSO-*d*₆): δ (ppm): 167.36 (C-OH), 158.89 (HC=N), 133.38 (aromatic), 131.95 (aromatic), 127.43 (aromatic), 118.87 (aromatic), 116.70 (aromatic), 69.89 (-CH(OH)-), 63.37 (-CH₂-), 20.38 (-CH₃). ESI-MS: m/z 327.3 $(C_{19}H_{22}N_2O_3 + H)^+$ (100%), 325.3 $(C_{19}H_{21}N_2O_3)^-$ (100%).

Conclusions

The complexes of copper(II) ions $[Cu_2L(CH_3COO)(CH_3OH)](CH_3OH)$ (1) and $[CuHL](CH_3OH)$ (2), where H_3L is N,N' -bis(5-methylsalicylidene)-2-hydroxy-1,3-propanediamine, were synthesized. In the presented dinuclear copper(II) ions, complex metal ions are 4-coordinate with almost ideally square-planar geometry and 5-coordinate with tetragonal pyramidal geometry. In the mononuclear complex, the copper ion is 4-coordinate, but the geometry is far from square-planar; rather, it can be described as extremely flattened tetrahedral. In both crystal

structures of copper(II) ion complexes, there are additional uncoordinated solvent methanol molecules. The methanol molecule in $[Cu_2L(CH_3COO)(CH_3OH)](CH_3OH)$ (1) is involved in the hydrogen-bonding system that connects the molecules of (1) into a three dimensional network. In $[CuHL](CH_3OH)$ (2), molecules of complex (2) are joined into infinite chains by means of O-H...O hydrogen bonds; the methanol molecules do not participate in the formation of these infinite chains. The ligand H_3L was found in two different crystalline forms: polymorphs A and B. Ligand H_3L A is the product of condensation reaction between 5-methylsalicylaldehyde and 2-hydroxy-1,3-propanediamine, whereas H_3L B is a product of template condensation reaction between 5-methylsalicylaldehyde and 2-hydroxy-1,3-propanediamine in the presence of lanthanide(III) ions. In both forms, H_3L molecules are essentially non-symmetric. The attempts to obtain the complex of lanthanide(III) ions (Dy(III), Tb(III)) and heterodinuclear complexes containing copper(II) ion and lanthanide (III) ions (Dy(III), Tb(III)) led to free ligand H_3L B and mononuclear complexes $[CuHL](CH_3OH)$ (2), respectively. The formation of complexes between N,N' -bis(5-methylsalicylidene)-2-hydroxy-1,3-propanediamine (H_3L) and Cu^{2+} , Tb^{3+} and Dy^{3+} ions was studied by pH-metry titration. It was found that copper(II) ion complexes exist in solid state as well as in solution, while the lanthanide(III) ion complexes formed only in solution.

The copper(II) complexes were found to be electroactive in voltammetric studies. These results showed the spectroelectrochemical behaviour of free ligand H_3L as well as the copper(II) complexes. The complexes showed both metal-centered and ligand-based colour changes.

Conflicts of interest

There are no conflicts to declare.

Acknowledgements

The financial support received from the National Science Centre, Poland (Grant No. 2016/21/D/ST5/01631) and from the Polish Ministry of Science and Higher Education (Grant No N N204 127 039) are gratefully acknowledged.

References

- (a) A. K. Asatkar, S. Panda and S. S. Zade, Thiophene-based salen-type new ligands, their structural aspects and dimeric Cu(II) complex, *Polyhedron*, 2015, **96**, 25–32; (b) I. G. Fomina, Z. V. Dobrokhotova, V. O. Kazak, G. G. Aleksandrov, K. A. Lysenko, L. N. Puntus, V. I. Gerasimova, A. S. Bogomyakov, V. M. Novotortsev and I. L. Eremenko, *Eur. J. Inorg. Chem.*, 2012, 3595–3610; (c) N. Kumar, A. K. Asatkar, S. Panda and S. S. Zade, Synthesis, characterization and supramolecular building motifs of substituted salphen- and thiasalphen-metal complexes, *Polyhedron*, 2016, **117**, 718–728; (d) Z. A. Taha, A. M. Ajlouni, W. A. Momani and A. A. Al-Ghazawi, Synthesis, characterization, biological activities and



- photophysical properties of lanthanides complexes with a tetradentate Schiff base ligand, *Spectrochim. Acta, Part A*, 2011, **81**, 570–577; (e) L. Rigamonti, A. Forni, M. Sironi, A. Ponti, A. M. Ferretti, C. Baschieri and A. Pasini, Experimental and theoretical investigations on magneto-structural correlation in trinuclear copper(II) hydroxido propellers, *Polyhedron*, 2018, **145**, 22–34.
- 2 (a) H. Wu, Y. Bai, Y. Zhang, G. Pan, J. Kong, F. Shi and X. Wang, Two lanthanide(III) complexes based on the Schiff base *N,N'*-bis(salicylidene)-1,5-diamino-3-oxapentane: synthesis, characterization, DNA-binding properties, and antioxidation, *Z. Anorg. Allg. Chem.*, 2014, **640**, 2062–2071; (b) Y. Sui, X.-N. Fang, R.-H. Hu, J. Li and D.-S. Liu, A new type of multifunctional single ionic dysprosium complex based on chiral salen-type Schiff base ligand, *Inorg. Chim. Acta*, 2014, **423**, 540–544.
- 3 (a) R.-X. Chen, T. Gao, W.-B. Sun, H.-F. Li, H.-F. Wu, M.-M. Xu, X.-Y. Zou and P.-F. Yan, Salen homonuclear and heteronuclear lanthanide(III) complexes with near-infrared (NIR) luminescence, *Inorg. Chem. Commun.*, 2015, **56**, 79–82; (b) L.-J. Wu, H. Yang, S.-Y. Zeng, D.-C. Li and J.-M. Dou, A family of hexanuclear lanthanide complexes with slow magnetic relaxation for Dy₆ cluster, *Polyhedron*, 2017, **129**, 77–81; (c) X. Yang, D. Lam, C. Chan, J. M. Stanley, R. A. Jones, B. J. Holliday and W.-K. Wohg, Construction of 1-D 4f and 3d–4f coordination polymers with flexible Schiff base ligands, *Dalton Trans.*, 2011, **40**, 9795–9801; (d) X. Yang, R. A. Jones, J. H. Rivers and W.-K. Wohg, Cyclic and acyclic oligo (N₂O₂) ligands for cooperative multi-metal complexation, *Dalton Trans.*, 2009, 10505–10510; (e) Y. Yue, P. Yan, J. Sun, G. Hou and G. Li, Structure and luminescent properties of 2D Salen-type lanthanide coordination polymers from the flexible *N,N'*-bis(salicylidene)-1,4-butanediamine ligand, *Polyhedron*, 2015, **94**, 90–95; (f) G. Feng, L. Yu-Yang, L. Cai-Ming, L. Yi-Zhi and Z. Jing-Lin, A sandwich-type triple-decker lanthanide complex with mixed phthalocyanine and Schiff base ligands, *Dalton Trans.*, 2013, **42**, 11043–11046.
- 4 (a) M. T. Kaczmarek, R. Jastrzab, E. Hołderna-Kędzia and W. Radecka-Paryzek, Self-assembled synthesis, characterization and antimicrobial activity of zinc(II) salicylaldehyde complexes, *Inorg. Chim. Acta*, 2009, **362**, 3127–3133; (b) M. Fleck, D. Karmakar, M. Ghosh, A. Ghosh, R. Saha and D. Bandyopadhyay, Synthetic aspects, crystal structure and antibacterial activity of two new Schiff base cobalt(III) complexes, *Polyhedron*, 2011, **34**, 157–162.
- 5 (a) P. G. Cozzi, Metal–Salen Schiff base complexes in catalysis: practical aspects, *Chem. Soc. Rev.*, 2004, **33**, 410–421; (b) F. Rajabi, A heterogeneous cobalt(II) Salen complex as an efficient and reusable catalyst for acetylation of alcohols and phenols, *Tetrahedron Lett.*, 2009, **50**, 395–397; (c) A. W. Kleij, Nonsymmetrical Salen Ligands and Their Complexes: Synthesis and Applications, *Eur. J. Inorg. Chem.*, 2009, **2**, 193–205; (d) L. F. Lima, M. L. Corraza, L. Cardoza-Filho, H. Márquez-Alvarez and O. A. C. Antunes, Oxidation of limonene catalyzed by metal(salen) complexes, *Braz. J. Chem. Eng.*, 2006, **23**, 83–92; (e) M. Azam, S. Dwivedi, S. I. Al-Resayes, S. F. Adil, M. S. Islam, A. Trzesowska-Kruszyska, R. Kruszynski and D.-U. Lee, Cu(II) salen complex with propylene linkage: an efficient catalyst in the formation of Csbnd X bonds (X = N, O, S) and biological investigations, *J. Mol. Struct.*, 2017, **1130**, 122–127; (f) P. Mahapatra, S. Ghosh, S. Giri, V. Rane, R. Kadam, M. G. B. Drew and A. Ghosh, Subtle Structural Changes in (Cu^{II})₂Mn^{II} Complexes To Induce Heterometallic Cooperative Catalytic Oxidase Activities on Phenolic Substrates (H₂L = Salen Type Unsymmetrical Schiff Base), *Inorg. Chem.*, 2017, **56**, 5105–5121; (g) Y.-L. Hou, S.-X. Li, R. W.-Y. Sun, X.-Y. Liu, S. W. Ng and D. Li, Facile preparation and dual catalytic activity of copper(I)-metallo-salen coordination polymers, *Dalton Trans.*, 2015, **44**, 17360–17365.
- 6 C. Papadopoulos, N. Kantiranis, S. Vecchio and M. Lalia-Kantouri, Lanthanide complexes of 3-methoxy-salicylaldehyde, *J. Therm. Anal. Calorim.*, 2010, **99**, 931–938.
- 7 (a) K. Das, S. Nandi, S. Mondal, T. Askun, Z. Cantürk, P. Celikboyun, C. Massera, E. Garribba, A. Datta, C. Sinha and T. Akitsu, Triply phenoxo bridged Eu(III) and Sm(III) complexes with 2,6-formyl-4-methylphenol-di(benzoylhydrazono): structure, spectra and biological study in human cell lines, *New J. Chem.*, 2015, **39**, 1101–1103; (b) P. Zhang, L. Zhang and J. Tang, Lanthanide single molecular magnets: progress and perspective, *Dalton Trans.*, 2015, **44**, 3923.
- 8 M. Layek, M. Ghosh, S. Sain, M. Fleck, P. T. Muthiah, S. J. Jennieffer, J. Ribas and D. Bandyopadhyay, Synthesis, crystal structure and magnetic properties of Nickel(II) and cobalt(III) complexes of a pentadentate Schiff base, *J. Mol. Struct.*, 2013, **1036**, 422–426.
- 9 R. Jastrzab, Studies of new phosphothreonine complexes formed in binary and ternary systems including biogenic amines and copper(II), *J. Coord. Chem.*, 2013, **66**, 98–113.
- 10 (a) X. B. Yang, Q. Wang, Y. Huang, P. H. Fu, J. S. Zhang and R. Q. Zeng, Synthesis, DNA interaction and antimicrobial activities of copper (II) complexes with Schiff base ligands derived from kaempferol and polyamines, *Inorg. Chem. Commun.*, 2012, **25**, 55–59; (b) R. Jastrzab, M. T. Kaczmarek, M. Nowak, A. Trojanowska and M. Zabiszak, Complexes of polyamines and their derivatives as living system active compounds, *Coord. Chem. Rev.*, 2017, **35**, 32–44.
- 11 H.-Y. Yin, J. Tang and J.-L. Zhang, Introducing metallosalens into biological studies: the renaissance of traditional coordination complexes, *Eur. J. Inorg. Chem.*, 2017, 5085–5093.
- 12 S. Saha, C. R. Choudhury, G. Pilet, A. Frontera and S. Mitra, *J. Coord. Chem.*, 2017, **70**, 1389–1405.
- 13 L. Lekha, R. K. Kanmani, R. Hariharan, M. Sathish, G. Rajagopal and D. Easwaramoorthi, *In vitro* antimicrobial and antioxidant evaluation of rare earth metal Schiff base complexes derived from threonine, *Appl. Organomet. Chem.*, 2015, **29**, 90–95.



- 14 G. Tircsó, Z. Garda, F. K. Kálmán, Z. Baranyai, I. Pócsi, G. Balla and I. Tóth, Lanthanide(III) complexes of some natural siderophores: a thermodynamic, kinetic and relaxometric study, *J. Inorg. Biochem.*, 2014, **127**, 53–61.
- 15 P. Mahapatra, S. Ghosh, S. Giri, V. Rane, R. Kadam, M. G. B. Drew and A. Ghosh, Subtle Structural Changes in $(\text{Cu}^{\text{II}}\text{L})_2\text{Mn}^{\text{II}}$ Complexes To Induce Heterometallic Cooperative Catalytic Oxidase Activities on Phenolic Substrates ($\text{H}_2\text{L} = \text{Salen Type Unsymmetrical Schiff Base}$), *Inorg. Chem.*, 2017, **56**, 5105–5121.
- 16 (a) R. Łyszczek and L. Mazur, Polynuclear complexes constructed by lanthanides and pyridine-3,5-dicarboxylate ligand: structures, thermal and luminescent properties, *Polyhedron*, 2012, **41**, 7–19; (b) C. Wang, S. Wang, L. Bo, T. Zhu, X. Yang, L. Zhang, D. Jiang, H. Chen and S. Huang, Synthesis, crystal structure and NIR luminescence properties of binuclear lanthanide Schiff Base complexes, *Inorg. Chem. Commun.*, 2017, **85**, 52–55.
- 17 *Rigaku Oxford Diffraction (2015) CrysAlis PRO (Version 1.171.38.41)*.
- 18 G. M. Sheldrick, A short history of SHELX, *Acta Crystallogr.*, 2008, **A64**, 112–122.
- 19 M. H. Irving, M. G. Miles and L. D. Petit, The stability constants of some metal chelates of triethylene-tetraminehexaacetic acid (ttha), *Anal. Chim. Acta*, 1967, **38**, 475–488.
- 20 P. Stańczak, M. Łuczowski, P. Juszczak, Z. Grzonka and H. Kozłowski, Interactions of Cu^{2+} ions with chicken prion tandem repeats, *Dalton Trans.*, 2004, 2102–2107.
- 21 P. Gans, A. Sabatini and A. Vacca, Investigation of equilibria in solution. Determination of equilibrium constants with the HYPERQUAD suite of programs, *Talanta*, 1996, **43**, 1739–1753.
- 22 L. Alderighi, P. Gans, A. Lenco, D. Peters, A. Sabatini and A. Vacca, Hyperquad simulation and speciation (HySS): a utility program for the investigation of equilibria involving soluble and partially soluble species, *Coord. Chem. Rev.*, 1998, **184**, 311–318.
- 23 (a) R. Jastrzab, Phosphoserine and specific types of its coordination in copper(II) and adenosine nucleotides systems – Potentiometric and spectroscopic studies, *J. Inorg. Biochem.*, 2009, **103**, 766–773; (b) R. Bregier-Jarzebowska, A. Gasowska, R. Jastrzab and L. Lomozik, Noncovalent interactions and coordination reactions in the systems consisting of copper(II) ions, aspartic acid and diamines, *Inorg. Biochem.*, 2009, **103**, 1228–1235.
- 24 T. Guo, Y. Guo, M. Guo, W. Chen and Y. Li, Synthesis and solid state structure of Schiff base copper(II) and Ni(II) complexes derived from *cis*-1,2-diaminocyclohexane, *Synth. React. Inorg. Met.-Org. Chem.*, 2015, **45**, 327–332.
- 25 (a) K. Andiappan, A. Sanmugam, E. Deivanayagam, K. Karuppasamy and H.-S. K. Dhanasekaran Vikraman, *In vitro* cytotoxicity activity of novel Schiff base ligand–lanthanide complexes, *Sci. Rep.*, 2018, **8**, 3054–3066; (b) M. Sedighipour, A. H. Kianfar, M. M. R. Sabzalin and F. Abyar, Synthesis and characterization of new unsymmetrical Schiff base Zn(II) and Co(II) complexes and study of their interactions with bovin serum albumin and DNA by spectroscopic techniques, *Spectrochim. Acta, Part A*, 2018, **198**, 38–50.
- 26 (a) W.-K. Dong, Y.-X. Sun, Ch.-Y. Zhao, X.-Y. Dong and L. Xu, Synthesis, structure and properties of supramolecular Mn^{II} , Co^{II} , Ni^{II} and Zn^{II} complexes containing Salen-type bisoxime ligands, *Polyhedron*, 2010, **29**, 2087–2097; (b) M. T. Kaczmarek, M. Kubicki and Z. Hnatejko, Two types of Lanthanide Schiff base complexes: synthesis, structure and spectroscopic studies, *Polyhedron*, 2015, **102**, 224–232.
- 27 (a) I. M. El-Deen, A. F. Shoaib and M. A. El-Bindary, Synthesis, structural characterization, molecular docking and DNA binding studies of copper complexes, *J. Mol. Struct.*, 2018, **249**, 533–545; (b) D. A. Edwards and R. N. Hayward, Transition metal acetates, *Can. J. Chem.*, 1968, **46**, 3443–3446; (c) G. Świdorski, M. Kalinowska, J. Malejko and W. Lweandowski, Spectroscopic (IR, Raman, UV and fluorescence) study on lanthanide complexes of picolinic acid, *Vib. Spectrosc.*, 2016, **87**, 81–87; (d) Y. Ouennoughi, H. E. Karce, D. Aggoun, T. Lanez, R. Ruiz-Rosas, B. Bouzerafa, A. Ourari and E. Morallon, *J. Organomet. Chem.*, 2017, **848**, 344–351.
- 28 (a) M. T. Kaczmarek, R. Jastrzab and M. Zabiszak, Complexes formation of lanthanide ions with *N,N'*-bis(5-methylsalicylidene)-4-methyl-1,3-phenylenediamine –potentiometric and spectroscopic studies, *J. Iran. Chem. Soc.*, 2018, **15**, 407–414; (b) M. T. Kaczmarek, R. Jastrzab and W. Radecka-Paryzek, Potentiometric study of lanthanide salicylaldimine Schiff base complexes, *J. Solution Chem.*, 2013, **42**, 18–26; (c) R. Hernández-Molina, A. Mederos, P. Gili, S. Dominguez, F. Lioret, C. Jano, M. Julve, C. Ruiz-Pérea and X. Solans, Dimer species in dimethyl sulfoxide–water (80 : 20 w/w) solution of *N,N'*-bis(salicylideneimine)-*m*-phenylenediamine ($\text{H}_2\text{sal-}m\text{-phen}$) and similar Schiff bases with Cu^{II} , Ni^{II} , Co^{II} and Zn^{II} . Crystal structure of $[\text{Co}_2(\text{sal-}m\text{-phen})_2]\cdot\text{CHCl}_3$, *J. Chem. Soc., Dalton Trans.*, 1997, 4327–4334.
- 29 E. S. Aazam, A. F. El Hussein and H. M. Al-Amri, Synthesis and photoluminescent properties of a Schiff-base ligand and its mononuclear Zn(II), Cd(II), Cu(II), Ni(II) and Pd(II) metal complexes, *Arabian J. Chem.*, 2012, **5**, 45–53.
- 30 D. F. Back, G. M. de Oliveira, L. A. Fontana, B. F. Ramão, D. Roman and B. A. Iglesias, One-pot synthesis, structural characterization, UV-Vis and electrochemical analyses of new Schiff base complexes of Fe(III), Ni(II) and Cu(II), *J. Mol. Struct.*, 2015, **1100**, 264–271.
- 31 A. Mishra, E. Mena-Osteritz and P. Bäuerle, Synthesis, photophysical and electrochemical characterization of terpyridine-functionalized dendritic oligothiophenes and their Ru(II) complexes, *Beilstein J. Org. Chem.*, 2013, **9**, 866–876.

